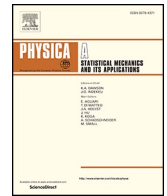




ELSEVIER

Contents lists available at ScienceDirect

Physica A: Statistical Mechanics and its Applications

journal homepage: www.elsevier.com/locate/physa

Dynamic analysis of transportation systems under small perturbations

Roberto Notari^a, Tarek Mudawar^b, Lorenzo Mussone^{c,*}^a Department of Mathematics, Politecnico di Milano, Via Bonardi, 9, Milano 20133, Italy^b ITIC School, CERM, Politecnico di Milano, Via Previati, 1/c, Lecco 23900, Italy^c Department ABC, Politecnico di Milano, P.za L. da Vinci, 32, Milano 20133, Italy

ARTICLE INFO

Keywords:

Dynamic analysis
 Transportation systems
 Centrality indices
 Graph
 Eigenvectors
 Equilibrium

ABSTRACT

In the present paper, we assess the dynamical response of a network under small perturbations that do not modify the network topology by means of a centrality index, called I_{centr} (see Section 3.1 and Mussone et al. (2022) [1] for its definition). In its design, this centrality index accepts weights on both nodes and edges, and so it can be iteratively applied, so to simulate a discrete linear dynamical system. It is associated to a suitable matrix \mathbf{M} , that depends only on the topology of the network and on the edge weights. We prove that the dynamical system converges, independent of the network, and compute the limit point. We apply it to a dataset of 34 underground transportation networks from cities throughout the world and investigate the convergence type of a single network and of a single node. We show that the nodes of the network tend to cluster according to their convergence type and that the convergence rate of a single network is exponential in the number of iterations. Furthermore, we show that the ratio $|\lambda_2/\lambda_1|$ where $|\lambda_1| \geq |\lambda_2|$ are the two largest module eigenvalues of \mathbf{M} , is suitable to compare the dynamical behavior of different networks.

1. Introduction

Efficient transportation networks are one of the cornerstones of urban societies. The efficiency of transportation systems encompasses a wide range of factors, from infrastructures and their maintenance to effective management, demand satisfaction, costs and reliability. The reliability of a transportation network is nowadays listed as robustness, resilience and vulnerability. Robustness is typically connected with the system's capacity to provide service in the face of disturbances, such as congestion, breakdowns or disruptions, no matter whether random failures or intentional attacks. The resilience is the ability of a system to adapt to and recover from disruptions in a timely manner. Finally, the vulnerability is the extent to which the transportation network is susceptible to extreme perturbations. In recent years, researchers have studied performance, robustness, resilience and vulnerability with techniques from graph theory and complex systems. After representing the transportation network as a graph, many different indices have been designed so to assess the feature under examination. One of the main criticalities of such studies is that it is difficult to consider the evolution on time of a transportation network, and to evaluate its performance under small or extreme perturbations (see Section 2 for a review of related literature). For what concerns the perturbation of a network, it is considered as equivalent to node or edge failure, and it is analyzed only under network topology changes. Indices to assess performance under perturbation are mainly elaborated on

* Corresponding author.

E-mail address: lorenzo.mussone@polimi.it (L. Mussone).

<https://doi.org/10.1016/j.physa.2026.131439>

Received 15 November 2025; Received in revised form 7 January 2026;

Available online 3 March 2026

0378-4371/© 2026 The Author(s).

<http://creativecommons.org/licenses/by/4.0/>.

Published by Elsevier B.V. This is an open access article under the CC BY license

the change of average path length and on clustering coefficient. However, a perturbation is not always associated to a change in the network topology, as mechanical systems show.

In the present paper, we address the following main research question: how can one evaluate the performance of a complex network under perturbations that do not modify the network topology?

To answer the question, we need a centrality index that can be used as a dynamical system, i.e. it must depend on both edge and node weights, so that one can iteratively compute it. To the authors knowledge, the only centrality index that fulfils such requirement is Icentr, introduced in Mussone et al. [1] and thoroughly described in Section 3.1. We show that it is suitable to analyze the network behavior under small or extreme perturbations that do not change the network topology. After computing the limit point of Icentr as dynamical system, we study the dynamical properties of 34 underground networks from cities all over the world. In details, we study

- the convergence type of a single node and
- the convergence rate of a single network.

Then, by leveraging on Icentr properties, we derive an index suitable to compare the dynamical behavior of different networks.

To shorten computations, following Derrible and Kennedy [2], we adopt a functional representation of underground networks (see Section 4.1). In addition to the Uniform Edge Weight (UEW) which emphasizes the topology of the network by setting the weight of each edge to one, we consider two more edge weights that capture the complexity of the entire networks: the Station Edge Weight (SEW), which uses the number of stations on each edge as edge weight, and the Distance Edge Weight (DEW), which uses the distance between nodes as weight for edges. The paper's most relevant findings are:

- Icentr can be computed as the product of a square matrix \mathbf{M} whose entries depend on the topology of the network and on the edge weights, and a column of the node weights (see Theorem 1),
- nodes with the same convergence type cluster in every network,
- the convergence rate of a network is exponential in the iteration number,
- the ratio between the module of the second largest eigenvalue and the largest one of \mathbf{M} is a good index for comparing the dynamical performance of different transportation networks.

The paper is organized as follows. In Section 2, we present a literature review on the topic of performance evaluation of transportation systems. In Section 3, we describe Icentr and prove its key properties other than a resume on the centrality indices Betweenness, Closeness, Degree and Eigenvector centrality. In Section 4, we apply Icentr to the 34 underground networks, first investigating the convergence type of a single node, then the convergence of a single network, and finally comparing the dynamical properties of the networks in the dataset. In Section 5, we present the key findings. Finally, we trace the conclusions in Section 6. Furthermore, the paper comprises three appendices: in Appendix A, we design the algorithm to efficiently compute Icentr, and estimate its computational complexity which turns out to be quadratic in the number of nodes; Appendix B contains two tables (Table B1 and Table B2) that contain the numbers of iterations Icentr requires to achieve a fixed convergence threshold for the networks in the dataset, by varying the initial edge weights and initial centrality index, in two different types of convergence calculation methods; -in Appendix C, Table C1 contains the eigenvalue ratios that evaluate the dynamical responses of the networks in the dataset for the three sets of edge weights.

2. Literature review

Robustness, vulnerability and resilience of networks have been widely applied to assess performance in the field of transportation. Since the importance of a reliable transport system is evident from an economic and welfare perspective, studies to assess and improve robustness and resilience of transportation networks have become increasingly numerous in recent years. King et al. [3] utilized quantitative metrics in graph theory to evaluate stations' impact on network resilience. Yang et al. [4] investigated the topological properties and resilience of the Beijing Subway system, introducing the Importance Evaluation Index to analyze node importance by combining the centrality measures Betweenness and Degree. Cats et al. [5] explored the robustness of complex network systems, focusing on disruptions or capacity limitations in Amsterdam's rail-bound transport networks. Zhang et al. [6] examined the resilience of the Shanghai Metro network, defining it in terms of post-disruption connectivity and rapid recovery using repair measures and employing the "resilience triangle" to quantify resilience loss. Sun et al. [7] analyzed the dynamic vulnerability of Beijing's subway network, utilizing a multi-static weighted method and complex network theory, introducing a model to assess dynamic vulnerability based on passenger flow.

Other than Betweenness, Closeness, Degree and Eigenvector, classical centrality indices, we quote the communicability distance, introduced in Estrada [8], as an attempt to consider small perturbations. Given two nodes, the communicability distance measures the amount of excitation at one of the two nodes transmitted to the other one. The author shows that summing up the contributions of all pairs of nodes is a graph invariant. This index has been applied to various complex networks to assess their robustness. In Cavallaro et al. [9], the authors studied the impact of small variations on the network topology on centrality metrics, In particular, Degree, Eigenvector and Katz centrality have been investigated under uniform or best connected scenarios of node failure.

From current research, it can be found that in-depth studies have been conducted on the static aspect of a network, and many achievements have been obtained. On the other hand, transportation networks evolve over time: considering to the time scale, changes can be observed in nodes and edges, in demand, in service level, or in the traffic flow, among the many others. This remark leads to the

study of temporal networks, that is to say, networks which take into account changes over time. Ducruet and Beauguitte [10] observed that network evolution and dynamics have been significantly underexplored, with a predominant focus on static approaches in existing studies. In the absence of concrete empirical data, several investigations have utilized simulation techniques to explore potential dynamic evolution for transport networks. Meng et al. [11] conducted a detailed investigation into the dynamic evolution of the Shenzhen Metro Network from 2004 to 2021. They aimed to analyze changes in network topology and node centralities over time. Using multiple network centrality indices, such as Degree, Eigenvector, Betweenness, and PageRank, they quantitatively assessed node importance across eight time periods. Zhang et al. [12] explored the dynamic characteristics of topology complexity within Nanjing's Weighted Metro Rail Transit Network, introducing the concept of time-varying characteristics of topology complexity dynamics. The study employed a network structure entropy based on station strength, which encapsulates the uniformity of energy distribution. Its availability is proved by conducting Pearson correlation analysis between it and a series of traditional weighted topology complexity indicators. Leng et al. [13] conducted a thorough analysis of the dynamic evolution of the Beijing Subway Network from 2007 to 2013, employing two modes: expanding and intensifying. They used a weighted network approach, strategically adding nodes and edges to assess network dynamics. Average degree, average shortest path length, and weighted clustering coefficient were employed in both modes to capture the dynamic evolution of the network. We refer to Zahoor et al. [14] for a review on the recent literature on temporal networks, not restricted to the transportation ones. As a further application, in Yunlong [15], temporal networks have been used in facing the problem of time series forecasting. As shown in Ali et al. [16], such a problem has a direct application to the traffic flow prediction, a quite challenging research field strictly connected to the design of smart cities. However, both perturbations in networks and temporal networks are always associated with topology changes in the network itself.

Over the past decades, iterative methods for computing eigenvalues have undergone remarkable advancements. Originating in the 1950s, seminal techniques like the Arnoldi/Lanczos method, independently developed by Arnoldi [17] and Lanczos [18], along with the Power Iteration method, dating back to the research of Householder [19], have played pivotal roles in solving eigenvalue problems with precision. However, despite their effectiveness, these methods found limited adoption in transportation research.

The transportation sector, characterized by complex network structures and dynamic operational environments, offers fertile ground for leveraging iterative eigenvalue methods. Notably, Meghanathan [20] employed principal eigenvalues of complex network graph adjacency matrices to assess variations in node degrees and their correlation with coefficient variations, while Chen and Tong [21] investigated graph dynamic evolution by examining changes in dominant eigen-pairs (eigenvalues and eigenvectors). However, these notable contributions remain scattered in transportation studies.

3. Methodology

Graph-based indices, particularly centrality indices, are essential tools for researchers to analyze networks. Each index emphasizes specific features of a transportation network while overlooking others. For instance, centrality indices focus on topological properties but often neglect important aspects of traffic, like time delay and vehicle flow. To capture the complex dynamics of transportation networks, we employ *Icentr*, a centrality index firstly introduced in Mussone et al. [1]. To the authors' knowledge, *Icentr* is the only centrality index that accepts weights on both edges and nodes, making it suited for studying the dynamics of transportation networks under perturbations that do not change the network topology, as we will demonstrate. Firstly, we describe the index and a set of centrality indices that supply the initial node weights. Secondly, we explain how to use *Icentr* to assess the dynamics of transportation networks.

3.1. Centrality indices

We start our review on centrality indices from *Icentr*, and then we recall definition and some features of Degree, Betweenness, Closeness, and Eigenvector centrality.

3.1.1. *Icentr*

Icentr (that is Index of Centrality) offers a metric for assessing transportation network efficiency by simultaneously considering both node and edge weights. The main principle underpinning *Icentr* is that a node is central if it is close to edges and nodes with great weight. The geometric idea is the following: assume that at time 0 one starts inspecting a network from a node. Then, at time 1, one reaches the neighbor nodes travelling along the edges containing the initial node and gains the aggregated contribution of the nodes and edges. At time 2, one arrives at the second neighbors along new edges or uses an edge connecting first neighbors and gains the aggregated contribution on the new edges and nodes, scaled by distance. Then, one iterates the procedure.

To fix notation, let us assume that the graph of interest is $G = (V, E)$, where V is the node set, and E is the edge set. Furthermore, we assume G to be simple and connected.

To calculate the value *Icentr* assigns at a node, one must sum the contribution of each edge of the graph; that is to say, if v is the node and e_1, \dots, e_r are the edges of G , we have

$$Icentr(v) = \sum_{i=1}^r ic(e_i). \quad (1)$$

where $ic(e)$ is a function defined in Eq. (3). To quantify the closeness of edges to the node v , we divide nodes and edges in levels: the smaller the level, the closer the node or the edge. The levels of nodes and edges are computed as follows.

- Node level: the node one is interested in, v in our notation, is the only level 0 node. Its neighbors are the level 1 nodes, and in general, a node is at level h if it is neighbor of a level $h-1$ node, and no other neighbor of it has smaller level.
- Edge level: as $e = \{i, j\}$, we have

$$\text{level}(e) = \begin{cases} \text{level}(j), & \text{if } \text{level}(i) < \text{level}(j); \\ 1 + \text{level}(i), & \text{if } \text{level}(i) = \text{level}(j); \\ \text{level}(i), & \text{if } \text{level}(i) > \text{level}(j). \end{cases} \quad (2)$$

The contribution of the edge $e = \{i, j\}$ that connects nodes i, j depends on the weights $w(i), w(j)$, of the nodes i, j and on the weight $w(e)$ of the edge e , and on their levels with respect to v , according to the following formula:

$$\text{ic}(e) = \begin{cases} \frac{w(i)}{2^{\text{level}(e)-1}} \times w(e), & \text{if } \text{level}(j) < \text{level}(i); \\ \frac{w(i) + w(j)}{2^{\text{level}(e)}} \times w(e), & \text{if } \text{level}(j) = \text{level}(i); \\ \frac{w(j)}{2^{\text{level}(e)-1}} \times w(e), & \text{if } \text{level}(j) > \text{level}(i). \end{cases} \quad (3)$$

The rationale behind Eq. (3) is the following. In case the nodes of the edge e have different levels, then we multiply the weights of the farther node and of the edge because the farther node is reached at the right time. In case the nodes have the same level, then we multiply the edge weight and the mean of the weights of the nodes. In all cases, we divide the product above by a suitable 2-power to consider the closeness to the starting node.

The number of levels is upper bounded by the diameter of the graph, that is generally small when the number of edges is close to its upper bound. E.g., for planar graphs, the number of edges does not exceed $3N - 6$, where N is the number of nodes.

The node weights can be chosen according to the aims of the study. When one assigns the Icentr values as node weights, Icentr becomes a dynamical system, capable of capturing the behavior of the network from a dynamical perspective without modifying the network topology. To guarantee convergence, the Icentr values must be normalized with respect to the l_2 vector norm which coincides with the Euclidean norm of vectors, since the node number is finite.

For the choice of the initial node weights, among the many possibilities, we recall the uniform weights (each node has the same weight), random weights, or the values of a centrality index as Degree, Betweenness, Closeness and Eigenvector Centrality. For reader's convenience, we recall the definitions of the four mentioned classical centrality indices.

3.1.2. Degree

Degree centrality, D , is a fundamental metric in network analysis that measures the importance of a node based on the number of its neighbors. Given the adjacency matrix $A = (a_{ij})$ of the graph G , where $a_{ij} = 1$ if $\{i, j\}$ is an edge, 0 otherwise, the Degree centrality of the node i is defined as

$$D(i) = \sum_{j \neq i} a_{ij}. \quad (4)$$

Graphs can generally be categorized into two types based on Degree centrality: those where a few nodes have exceptionally high degrees, forming a hub structure, and those where most nodes have similar degrees.

3.1.3. Betweenness

To evaluate the role of a node in facilitating information transmission between any two nodes inside the network, Freemann [22] introduced the Betweenness centrality, which was later refined by various researchers. The main basics underpinning Betweenness is that a node is central when it belongs to many of the shortest paths between node pairs. The Betweenness centrality $B(v)$ of a node v is then calculated as:

$$B(v) = \sum_{s \neq v \neq t} \frac{\sigma_{st}(v)}{\sigma_{st}} \quad (5)$$

where $\sigma_{st}(v)$ is the number of shortest paths from s to t through v , and σ_{st} is the total number of shortest paths from s to t .

To enhance interpretability and standardize the centrality within the $[0,1]$ range, researchers tend to normalize it by $(N - 1)(N - 2)/2$, where N is the number of nodes in the graph. This normalization allows for a more intuitive understanding of the centrality measure of the nodes.

For large scale networks, the algorithm for computing the Betweenness centrality has a complexity of $O(N^3)$ thus making it impractical [23]. Recognizing this challenge, a more efficient algorithm was introduced by Brandes [24], reducing the complexity to $O(N^2)$ allowing the computation of Betweenness for large networks.

3.1.4. Closeness

Originating from Bavelas [25], Closeness centrality assesses the importance of a node by considering the lengths of geodesic (that is to say, shortest path) from it to all other nodes in the network. The definition of the (normalized) Closeness of a node v is:

$$C(v) = \frac{N - 1}{\sum_{u \neq v} d(u, v)} \tag{6}$$

where N is the number of nodes in the graph, and $d(u, v)$ is the length of the shortest path from u to v .

3.1.5. Eigenvector centrality

The fourth centrality measure we consider is Eigenvector centrality. The criterion behind its design is that a node is central if its neighbors are so (e.g., see Piraveenan and Saripada [26]). This criterion is rooted in the principal eigenvector of the adjacency matrix of the network, emphasizing the impact of well-connected neighbors, as defined in Bonacich [27].

Mathematically, given the adjacency matrix A of the graph G and a vector $X = (x_1, \dots, x_n)$ storing the centrality scores, the Eigenvector centrality of the i th node satisfies:

$$\lambda x_i = a_{i1}x_1 + a_{i2}x_2 + \dots + a_{iN}x_N, i = 1, \dots, N. \tag{7}$$

In matrix form, if λ is the largest eigenvalue of the adjacency matrix, the equality above becomes

$$\lambda X = AX. \tag{8}$$

It is well known that the eigenvector associated with the largest eigenvalue has positive coordinates.

3.2. Icentr as a dynamical system

As explained in the Icentr definition, Icentr can be used as a dynamical system as follows

$$\begin{cases} Y_t = X_t / \|X_t\| \\ X_{t+1} = \text{Icentr}(Y_t) \end{cases} \tag{9}$$

where we use the Euclidean norm for vectors, and the argument of Icentr function is a vector of node weights. The node weights from which the computation starts are which are obtained from a centrality index like Degree, Betweenness, Closeness or Eigenvector centrality, or can be randomly or uniformly chosen. Hence, the Icentr function depends on the edge weights which are fixed at the beginning and cannot be changed during the calculation. The first property on which we focus is the form of the Icentr function.

Theorem 1. *Given a simple connected graph with N nodes, there exists an $N \times N$ matrix M with non-negative entries that depends on the graph G and on the edge weights, such that*

$$\text{Icentr}(Y_t) = M Y_t. \tag{10}$$

Proof. According to the Icentr definition, the value at a node is the sum of the contributions of all edges, and these last values are the products of edge weights and node weights, divided by a suitable-power whose exponent depends on the edge level. So, if we accumulate the node weights, we have

$$\text{Icentr}(i) = \sum_{j \in V} m_{ij} w(j). \tag{11}$$

Assume j is a node different from i . Then, its level is $h \geq 1$ and hence there exists a level $h - 1$ node k that is a neighbor of j ; that is to say, there is an edge $e = \{j, k\}$ whose level is $level(j)$, and soAs i is the only level 0 node, its weight never multiplies the weight of an edge to assess the contribution of an edge. It follows that for every node i , and this completes the proof. QED

From the Perron-Frobenius theorem, the matrix M above has a real, positive, simple eigenvalue λ that is larger than the modulus of every other eigenvalue of M . Moreover, we can assume the associated eigenvector to have positive entries. From the point of view of a dynamical system, we have

Proposition 2. *Let \bar{v} be the positive eigenvector associated to λ . Then,*

$$\lim_{t \rightarrow +\infty} Y_t = \frac{\bar{v}}{\|\bar{v}\|}. \tag{12}$$

Proof. Let \bar{w} be a left eigenvector associated to M with respect to λ , that is to say, $\bar{w}^T M = \lambda \bar{w}^T$. From the Perron-Frobenius Theorem, it follows that

$$\lim_{t \rightarrow +\infty} \frac{M^t}{\lambda^t} = \bar{v} \bar{w}^T. \tag{13}$$

Since $Y_1 = \frac{M X_0}{\|M X_0\|}$, $X_2 = M Y_1 = \frac{M^2 X_0}{\|M^2 X_0\|}$, $Y_2 = \frac{X_2}{\|X_2\|} = \frac{M^2 X_0}{\|M^2 X_0\|}$, by iterating we get $Y_t = \frac{M^t X_0}{\|M^t X_0\|}$.

Then, we have

$$\lim_{t \rightarrow +\infty} Y_t = \lim_{t \rightarrow +\infty} \frac{\mathbf{M}^t X_0}{\|\mathbf{M}^t X_0\|} = \lim_{t \rightarrow +\infty} \frac{\frac{\mathbf{M}^t}{\lambda^t} X_0}{\left\| \frac{\mathbf{M}^t}{\lambda^t} X_0 \right\|} = \frac{\bar{v} \bar{w}^T X_0}{\|\bar{v} \bar{w}^T X_0\|} = \frac{\bar{v}}{\|\bar{v}\|}, \tag{14}$$

since $\bar{w}^T X_0$ is a positive number because both \bar{w} and X_0 have positive entries. QED Hence, the limit point of the dynamical system associated with Icentr depends uniquely on the matrix \mathbf{M} , and so on the topology of the graph and on the edge weights.

To assess the dynamical properties of the graph, we study the rate of convergence of Y_t to the normalized eigenvector of \mathbf{M} associated to λ .

In [Appendix A](#), we provide an algorithm to compute Icentr at each node and evaluate its computational complexity. The procedure can be easily modified so that it provides the matrix \mathbf{M} of [Theorem 1](#) at its first run. Hence, the computation of Icentr values reduces to a matrix-vector multiplication, whose computational complexity is $N(N - 1)$, slightly smaller than the complexity of the Icentr procedure.

3.3. Dynamical assessment

To evaluate the dynamical properties of a graph, we study the rate of convergence of to the normalized eigenvector \bar{v} in two different ways.

The first one, the Icentr Convergence Method, ICM for brief, consists in iteratively computing Y_t until the l_2 norm of $Y_{t+1} - Y_t$ is less than a given threshold. The second one, the Eigenvector Convergence Method, ECM for brief, consists in iteratively computing Y_t until the l_2 norm of $Y_t - \bar{v}$ is less than a given threshold. The comparison of the number of iterations allows us to inspect the graph dynamics.

The correctness of the second method is based on [Proposition 2](#) and the Power Iteration method for the computation of the eigenvector associated to the largest eigenvalue, by von Mises [\[28\]](#), Householder [\[29\]](#), and von Neumann [\[30\]](#). Note that the computation of \bar{v} from the matrix \mathbf{M} is not investigated in this paper.

A crucial aspect of both methods is the normalization of Icentr vector after each application of the Icentr function to ensure stability and convergence.

4. Applications

4.1. Graphs associated with underground networks

To show the potential of the methodology exposed in the previous section, we study thirty-four metro networks worldwide from the

Hong Kong underground network

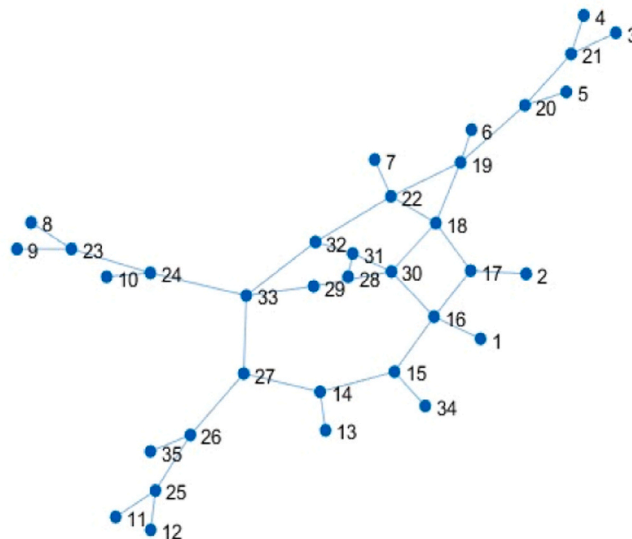


Fig. 1. Functional representation of Honk Kong underground network: only terminals and hubs are reported as nodes. The network consists of a central core, and legs attached to it; the legs do not contain cycles, so they are trees in a graph-theoretical setting. The core contains two cycles with 3 edges, one with 4, two with 5, and one with 7 edges. The presence of a cycle with 7 edges makes Hong Kong network almost unique in the analyzed dataset.

dynamical perspective. The first step consists in associating a graph to each metro network. In constructing the corresponding undirected graph $G = (V, E)$ for each network, we adopt the following rule: only terminals and transfer stations are nodes, whereas the rail tracks are represented as undirected links. Intermediary stations with only two connections, termed passing stations, are removed from the graph's node set to focus on network topology and reduce the computational burden. According to Derrible and Kennedy [2], such a representation is called functional, to distinguish it from the full, where every station is a node. To get the functional graph from the full one, one must remove degree 2 nodes, one at a time, and insert an edge that substitutes the node and the two edges containing it. Since we want the functional graph to be simple, that is to say, it does not contain loops and multiple edges, we do not remove a degree 2 node if its cancelation produces a multiple edge. Moreover, when a terminal node is connected to two lines, a fictitious node is added and connected to the terminal. While constructing weighted graphs, the length of the fictitious links is set to one kilometre. As example, we report the functional representation of Hong Kong metro network (Fig. 1).

Once the graph that represents the metro network has been constructed, we set weights for edges as follows. The first weight of an edge is 1, for every edge, to highlight the graph topology. We refer to these weights as UEW (Uniform Edge Weights). The second weight of an edge is two plus the number of stations that have been removed in the passage from the full to the functional graph. These weights highlight the importance of the edge in the network from the point of view of the passenger flow. We refer to these weights as SEW (Station Edge Weights). The third and last weight of an edge is its length, computed in kilometres. These weights highlight the importance of the edge in the network from a metric perspective. We refer to these weights as DEW (Distance Edge Weights).

For reader's convenience, we recall that the length of a path is the sum of the weights of the edges in the path, while the distance between two nodes is the minimum length of a path connecting the two nodes. Hence, distances depend on edge weights. Finally, the diameter is the maximum distance between two nodes in the graph. As previously said, UEW diameter is an upper bound for the number of levels in the Icentr procedure. In Table 1, we summarize information about the networks in the dataset.

Before analysing the convergence of Icentr, we make some remarks about the networks in the dataset. The graphs that represent the considered underground networks are all planar. Furthermore, the number of edges E is in the range $[N, 1.69N]$, where N is the number of nodes in the graph. Since the upper bound for E in a planar graph is $3N - 6$, the number of edges is relatively small with respect to the number of nodes, making the graphs not particularly dense. Also, we can split the dataset in three parts, according to the number of nodes:

- the first subset contains 11 graphs with $7 \leq N \leq 13$ nodes: the number of edges verifies $N \leq E \leq 1.17N$,

Table 1

List of cities in the dataset with their corresponding basic topological characteristics (UEW: Uniform Edge Weights; SEW: Station Edge Weights; DEW: Distance Edge Weights;).

Underground Networks	Number of Nodes	Number of Edges	Average Degree	UEW Diameter	SEW Diameter	DEW Diameter
Athens	12	14	2.33	5	37	46.26
Barcelona	36	54	3.00	10	39	33.02
Beijing	78	121	3.10	12	68	101.00
Berlin	34	45	2.65	8	55	37.57
Boston	29	34	2.34	8	45	37.19
Brussels	9	10	2.22	4	34	17.91
Bucharest	13	14	2.15	6	25	24.97
Buenos Aires	18	24	2.67	5	28	16.79
Cairo	12	14	2.33	5	38	41.60
Chicago	19	19	2.00	7	50	50.64
Delhi	45	59	2.62	10	76	73.90
Hong Kong	35	39	2.23	10	32	66.15
Lisbon	13	15	2.31	4	25	17.75
London	75	112	2.99	12	56	78.85
Lyon	10	10	2.00	4	21	13.07
Madrid	56	90	3.21	12	59	63.99
Marseilles	7	7	2.00	3	19	11.73
Mexico City	42	62	2.95	9	42	41.89
Milan	21	24	2.29	6	41	34.90
Montreal	11	12	2.18	4	33	24.31
Moscow	65	106	3.26	11	38	54.53
New York	85	124	2.92	13	76	62.71
Osaka	39	51	2.62	9	51	73.53
Paris	86	136	3.16	13	51	26.60
Prague	9	9	2.00	3	26	25.10
Rome	10	10	2.00	4	38	31.05
Saint Petersburg	17	20	2.35	5	24	33.56
Seoul	119	194	3.26	15	87	205.90
Shanghai	88	142	3.23	13	57	116.20
Singapore	34	57	3.35	7	39	47.03
Stockholm	20	20	2.00	7	42	37.70
Tokyo	65	110	3.38	11	39	39.20
Toronto	12	12	2.00	5	40	39.62
Washington	26	32	2.46	7	38	76.65

- the second subset contains 14 graphs with $17 \leq N \leq 45$: the number of edges verifies $N \leq E \leq 1.69N$,
- the third and last subset contains 9 graphs with $56 \leq N \leq 119$: the number of edges verifies $1.46N \leq E \leq 1.69N$.

Hence, the graphs in the first subset have nearly identical numbers of nodes and edges, the ones in the third subset have almost the number of edges equal to 1.5 of the number of nodes. Finally, the graphs in the second subset are the most scattered. Another remark concerns the distribution of the graphs in the range $[\min(N), \max(N)] = [7, 119]$: about half of the graphs verify $N \leq 26$, and so the dataset is far from being equally distributed. The diameter of the graphs with respect to UEW is well fitted by a degree 2 polynomial in the number of nodes.

This is fairly surprising, especially when compared to the diameters with respect to SEW or DEW which exhibit no specific feature. In the next subsections, we consider the convergence of a single node in a network, the convergence of a network, and finally, a comparison of convergence rates between different networks (Figs. 2-4).

4.2. Node and network convergence

In this section, we examine a single network and address the following research questions. Since we proved in Proposition 2 that the normalised Icentr values converge to the Perron-Frobenius normalised positive eigenvector of the matrix M which depends only on the graph topology and on the edge weights, we can explain the dynamical system associated with Icentr in terms of equilibrium and small perturbations. Hence, one can investigate the way:

1. a single node gets its final value,
2. the Icentr iterates converge to the Perron-Frobenius eigenvector.

When looking at a single node, the convergence can be of three different characters: increasing, oscillating, and decreasing. With increasing (decreasing, respectively), we mean that $Y_t(v) \leq Y_{t+1}(v)$ ($Y_t(v) \geq Y_{t+1}(v)$, respectively) for every iterate t . With oscillating, we mean that the sequence $\{Y_t(v)\}$ does not satisfy any of the two previous constraints.

For networks with a limited number of nodes N , most of the node values oscillate to reach the final value. As shown in Fig. 5, the same node can converge in different manners when the initial value or the weights change. However, nodes with the same convergence dynamics tend to cluster near together, with oscillating nodes that separate the two sets. We demonstrate this phenomenon for the Honk Kong network (Fig. 6), but the same applies to all other networks in the dataset.

4.3. Dynamical response of a network

Since both the Icentr iterates and the Perron-Frobenius eigenvector are normalized, we can compute both the norm of the difference, and the angular distance between every single Icentr iterate and the Perron-Frobenius eigenvector, in the three cases of Uniform, Distance and Stations weights. Since the results are very similar for all networks in the dataset, we only report figures for the

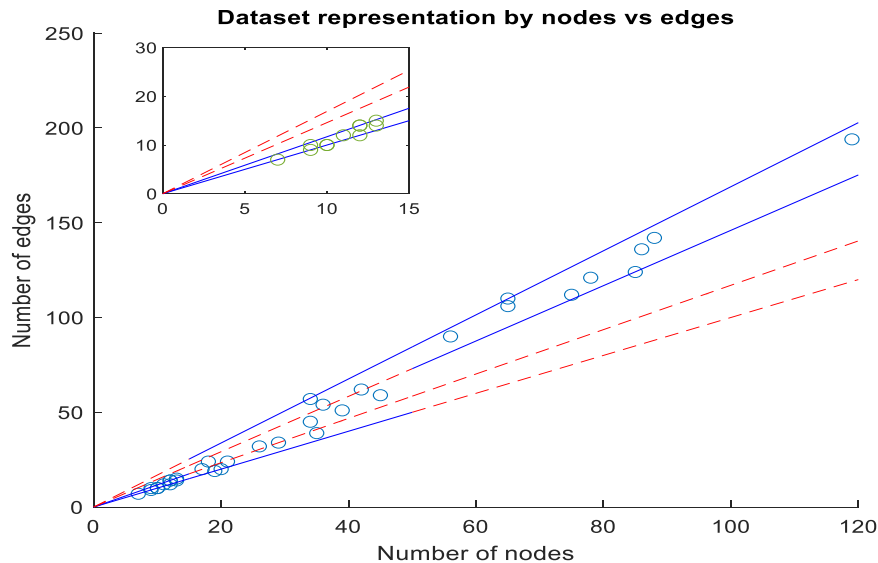


Fig. 2. The points have coordinates (v, e) , where v is the number of nodes and e is the number of edges in a graph in the dataset. The blue and red lines have equation $e = v$, $e = 1.17v$, $e = 1.46v$, and $e = 1.69v$. Graphs with at most 13 nodes (expanded in the small box) lie in between the two lines with least slopes. Graphs with nodes in the range $[17, 45]$ are spread between the two external lines. Graphs with at least 56 nodes are in between the two lines with largest slopes. It is evident that most graphs verify $v \leq 26$.

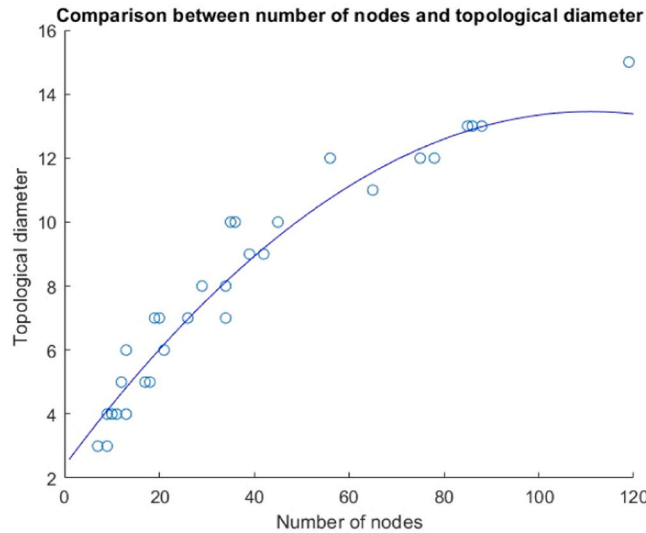


Fig. 3. The points have coordinates $(N, Diam)$ where N is the number of nodes and $Diam$ is the diameter of the graph with respect to the uniform weight of edges. The blue curve has equation $Diam = -0.0009N^2 + 0.1996N + 2.3841$ and is the best fitting degree 2 polynomial curve. The errors are, respectively, $SSE = 19.109$, $R\text{-square} = 0.95104$, $Adj\ R\text{-square} = 0.94788$, $RMSE = 0.78513$.

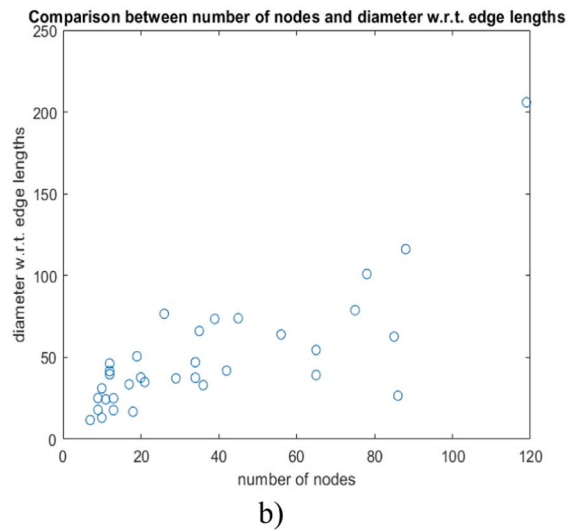
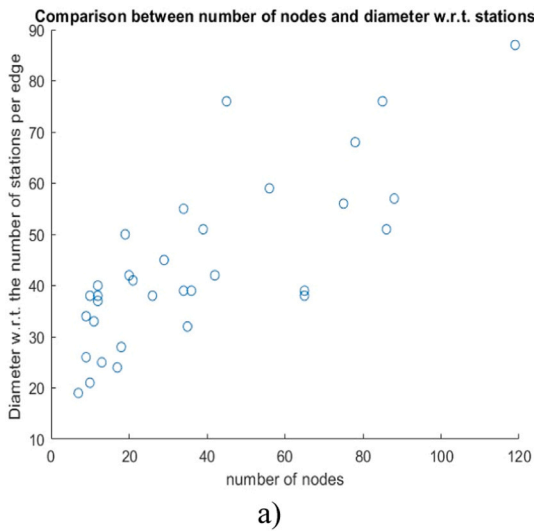


Fig. 4. On the left (a), the points have coordinates $(N, Diam)$ where the diameter is the number of stations on each edge. On the right (b), the points have coordinates $(N, Diam)$, where the diameter is computed by summing up the lengths of each edge. In both cases, the two clouds have no evident feature.

Hong Kong network, whose layout has already been reported in Fig. 1. From those figures (Fig. 7), the role of weights is evident, since we get similar but not equal figures. In all cases, asymptotically, the convergence of Icentr iterates Y_t to the Perron-Frobenius eigenvector v is exponential in the iteration number, that is to say, asymptotically, we have $\|Y_t - v\| = c_1 e^{-m_1 t}$ for suitable c_1, m_1 that depend on the centrality index chosen as starting point, and on the edge weights. The angle between Y_t and v asymptotically behaves in a similar way.

If we take a descriptive statistics approach, we must analyze how the average value and standard deviation of the Icentr iterates converge to the ones of the Perron-Frobenius eigenvector. As Fig. 8 show, the average value and the standard deviation of Icentr iterates become essentially equal to the ones of the Perron-Frobenius eigenvector after about 8 iterations. This number of iterations is about equal to which the logarithm of the norm of the difference becomes linear in the number of iterates, as shown Fig. 7a. Moreover, Fig. 8a and Fig. 8b have opposite shape: the trajectory that starts from Eigenvector centrality is the only that approaches the average (resp. the standard deviation) of the Perron-Frobenius eigenvector from below (resp. from above). It is worthwhile to examine the initial iterations, because what happens during the second iterate determines the general pattern of convergence.

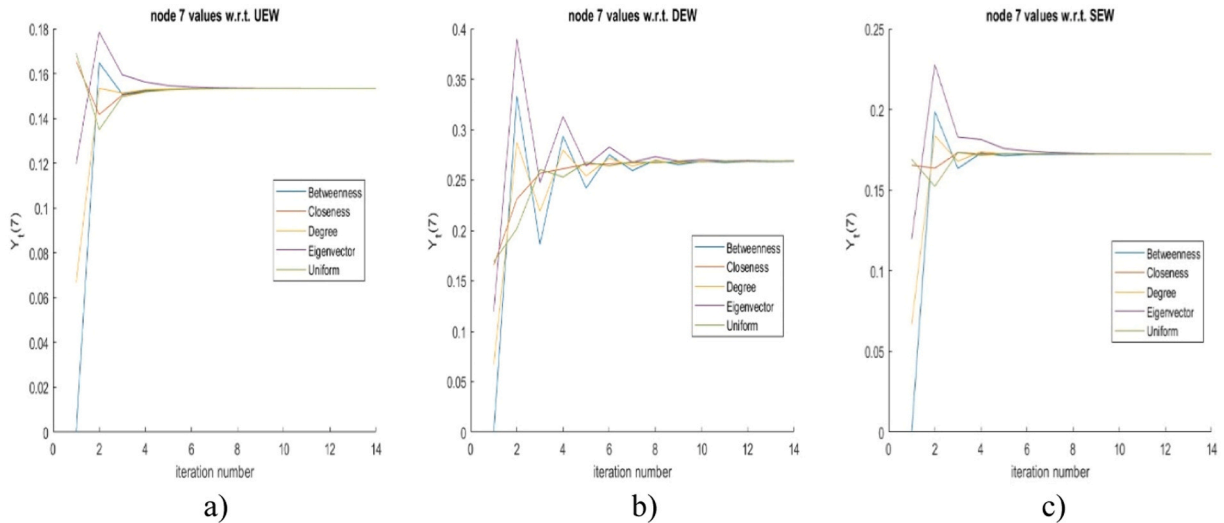


Fig. 5. In the 3 figures (a–c), we show the values of the Icentr iterates at node 7 of Honk Kong metro network (Fig. 1), with respect to weights UEW (a), DEW (b), and SEW(c), respectively. After the first 3 iterates, the convergence to the final value is monotonic if we consider UEW, either decreasing, or increasing. For DEW, the values of the iterates mostly oscillate around the final value. Finally, for SEW, we have an intermediate situation: oscillations for some starting indices, a monotonic trend for the others.

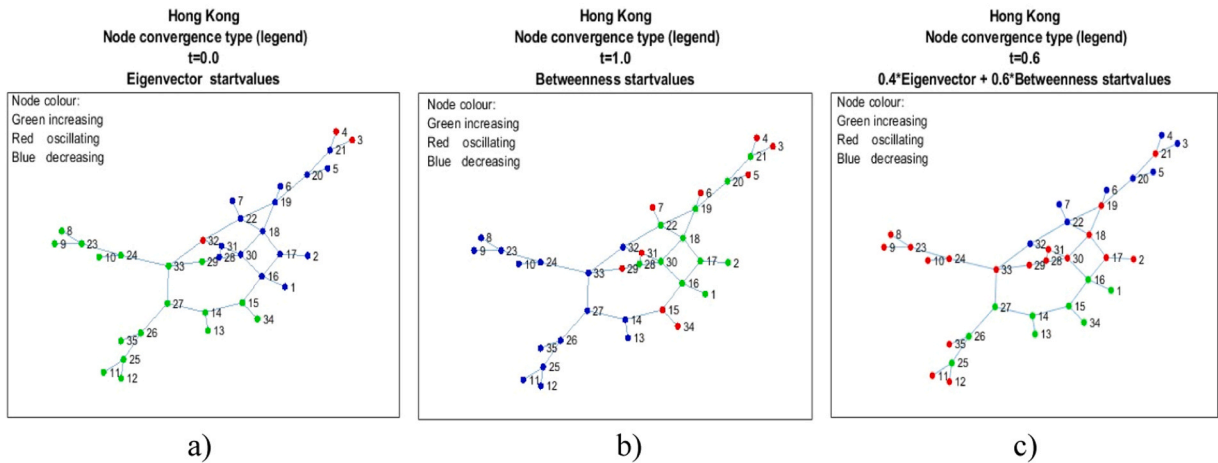


Fig. 6. In the three figures (a–c), the color of a node indicates the convergence type: green nodes converge increasingly to the final value, blue ones converge decreasingly, and red nodes oscillate. We consider the Hong Kong metro network with UEW in all of them. In the left picture (a), we use Eigenvector centrality as starting values, in the central one (b), we use Betweenness. It is noteworthy that the convergence type switches from increasing to decreasing and conversely in the two pictures. When considering a mixture of the two indices (0.4 Eigenvector + 0.6 Betweenness), we get the transition (c).

4.4. Comparison between the number of iterations

Finally, we analyze the number of iterations required to achieve the threshold, set to 10^{-5} in all computations, when using either ICM or ECM methods. Of course, that number depends on the centrality index that fixes the starting point, on the topology of the network itself, and on the edge weight because of the use of Icentr. We report in Table 2 the number of iterations for both methods, all five centrality indices and the three edge weights for Hong Kong metro network.

The number of iterations for all networks in all considered cases is reported in Appendix B. We report some statistics concerning the role of the edge weight in the following Table 3. To that end, we merge all data for the five centrality indices into one dataset for each edge weight.

When comparing the number of iterations to get the threshold for ICM and ECM, we have that the correlation coefficient between the outcomes of the two methods when starting from the same initial node weights, is very large. We report those correlation coefficients in Table 4. When employing UEW (DEW, SEW, respectively), the highest correlation occurs when starting with Closeness

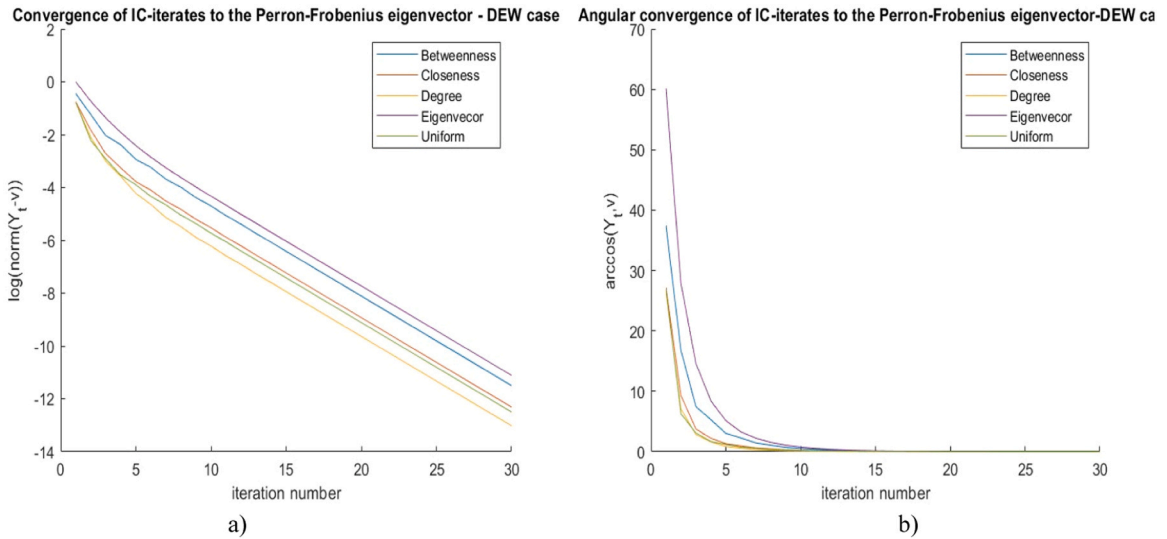


Fig. 7. These figures report the log of the norm of the difference between Icentr iterates and Perron-Frobenius eigenvector (a) and the arccos of them (b) for the DEW case of Hong Kong network; very similar pictures are obtained for the other networks. When comparing this case with UEW and SEW cases, we remark that (i) the convergence is slower; (ii) Eigenvector centrality is the farthest and the slowest to converge to the Perron-Frobenius eigenvector v .

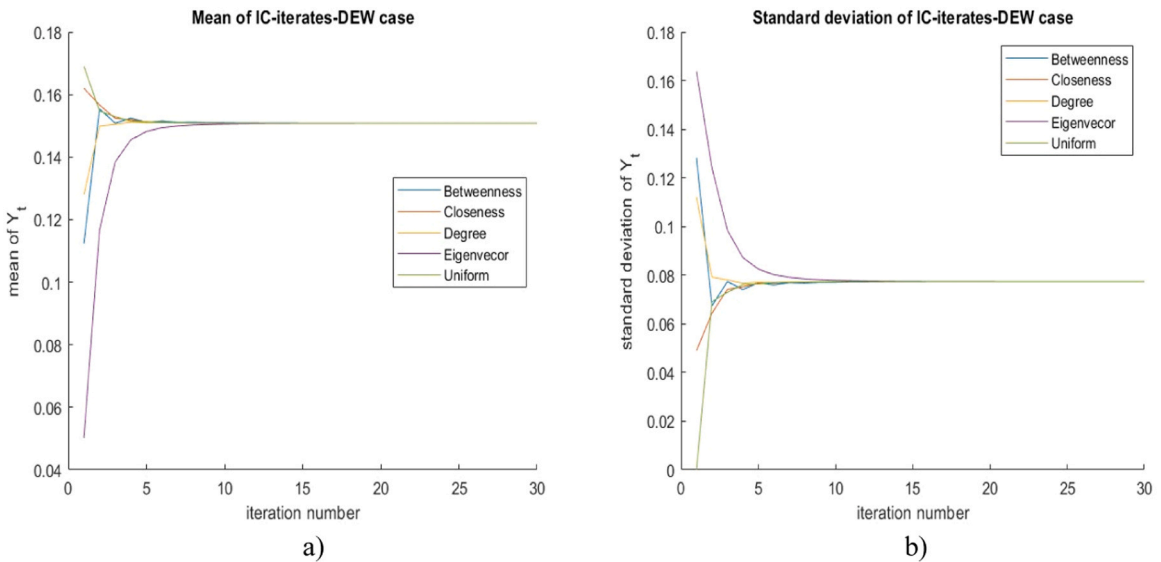


Fig. 8. In these figures, we report the mean (a) and the standard deviation (b) of each Icentr iterate Y_t in the DEW case, for the Hong Kong network, since the other cases are similar. It is evident that the convergence of the mean value of the Icentr iterates is monotonic, but Eigenvector centrality behaves the opposite of the other four centrality indices. The same happens for the standard deviation. The role of the weights emerges because Eigenvector centrality has the smallest mean in two cases over three, and the part of the picture where there are more fluctuations is different from case to case.

(Uniform, Eigenvector centrality, respectively). In contrast, the smallest correlation occurs when starting from Betweenness in the UEW case, from Betweenness when using SEW, and from Degree in the DEW case.

In analysing the number of iterations, we have computed for each network, their average number across the five centrality indices and compared it to the number of nodes of the graph. The outcome in the case of UEW is reported in Fig. 9.

5. Results

In this section, we present the results of the three types of analyses we conducted on the dataset, in the same order as in the previous

Table 2

Number of iterations for ICM and ECM for the Hong Kong graph in the UEW, SEW, and DEW cases. For this network, when one starts from Eigenvector centrality, one needs always more iterations. This is not the general feature: the centrality index that needs more iterations or less iterations, changes according to the network and to the edge weight.

Hong Kong	Betweenness	Closeness	Degree	Eigenvector	Uniform
ICM-UEW	13	13	12	14	13
ECM-UEW	13	12	12	13	13
ICM-SEW	13	14	14	17	10
ECM-SEW	13	14	14	17	10
ICM-DEW	27	24	22	28	24
ECM-DEW	30	27	25	31	27

Table 3

Statistics for the two convergence methods and for the three edge weights. It is evident that the Station Edge Weight has an intermediate effect between the Uniform Edge Weight and the Distance Edge Weight, on the networks in the dataset.

	ECM			ICM		
	UEW	DEW	SEW	UEW	DEW	SEW
MIN	4	8	8	5	9	9
MAX	22	293	42	21	209	39
MEAN	10,43	31,65	16,22	10,43	27,85	16,17
MEDIAN	9	20	14	10	20	14
MODE	7	13	13	8	14	14

Table 4

Correlation coefficients between the number of iterations to get the threshold for ECM and ICM when starting from the same centrality index, for the three edge weights for the Hong Kong network. Even if we do not report the correlation coefficients for all networks in the dataset, they have similar magnitude.

	Betweenness	Closeness	Degree	Eigenvector	Uniform
UEW	0.9893	0.9939	0.9936	0.9929	0.9937
DEW	0.9986	0.9984	0.9968	0.9979	0.9989
SEW	0.9894	0.9907	0.9910	0.9979	0.9946

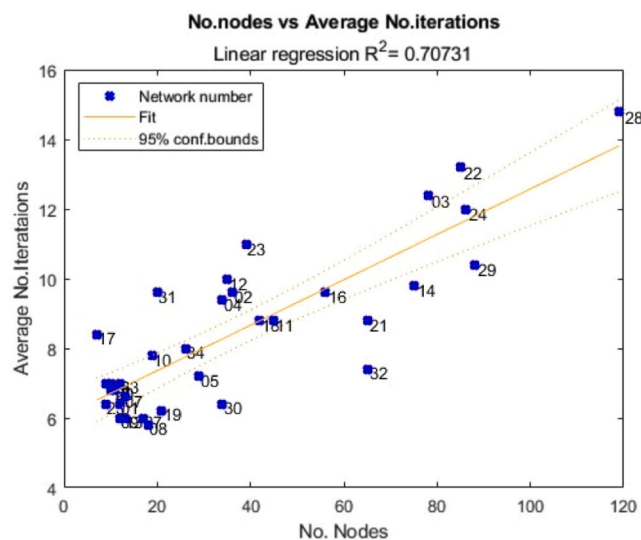


Fig. 9. We have plotted the number of nodes for each network against the average number of iterations across the five centrality indices, in the UEW case. The number of the blue dots corresponds to the network node number as in Table 1. Even if the blue dots are relatively sparse, it is evident a tendency to move up along the y-axis as the number of nodes increases. The outcomes in the DEW and SEW cases are similar.

section. When we consider a single node, we observed that the convergence type (increasing, decreasing, oscillating) depends on the starting values of nodes and on the edge weights. It is noteworthy that when we use Eigenvector centrality as starting values and a node converges in an increasing way, then the same node generally converges in a decreasing way when using the other four starting values, namely Betweenness, Closeness, Degree, and Uniform, and conversely, with computations done by one among UEW, DEW or SEW. This feature shows that, given an edge weight, the space of vectors with modulus one can be divided into different regions, according to the convergence type of nodes, and that Eigenvector centrality and the other four indices belong to distinct regions. Mixtures between Eigenvector centrality and one of the other starting values can be used to determine the border between those regions. In all experiments we performed, the border is only crossed once (see Fig. 6).

Since we use Icentr to evaluate the dynamic response of a network, we perform also the following experiments: we compute the normalized Perron-Frobenius eigenvector, then we perturb the value at one node only and we use those perturbed values as starting values for the Icentr procedure. The number of iterations to reach the normalized Perron-Frobenius eigenvector is independent on the node and on the network, and varies in the range [2, 5] when we use UEW. Furthermore, the convergence type of nodes depends on the perturbation, as follows. The perturbed node always oscillates around the convergence value. For the remaining nodes we have that, if one of them has increasing convergence type when we increase the value at the perturbed node, then it has decreasing convergence type when we decrease that value, and conversely. See Figs. 10 and 11 for an illustration of the previous feature in the case of Hong Kong network.

Now, we consider the convergence of the Icentr iterates to the Perron-Frobenius positive eigenvector. In Section 4.2, we remarked that, asymptotically, the convergence is exponential, independently from the network. E.g., we have $\|Y_t - v\| = c_1 e^{-m_1 t}$ for suitable c_1, m_1 that depend on the centrality index chosen as starting point, and on the edge weights, where Y_t is the normalized Icentr iterate and v is the normalized positive Perron-Frobenius eigenvector.

The angle between Y_t and v asymptotically behaves in a similar way: indeed, from the properties of the scalar product, we have:

$$\|Y_t - v\|^2 = \|Y_t\|^2 + \|v\|^2 - 2 \|Y_t\| \|v\| \cos \widehat{Y_t v}. \tag{15}$$

Since Y_t and v have norm 1, for t sufficiently large the angle $\widehat{Y_t v}$ is small, so that we can use the McLaurin approximation at the second order. Hence, we get

$$\|Y_t - v\| = \widehat{Y_t v} \tag{16}$$

and this shows that the norm and the angle have the same asymptotic behavior. So, the interesting part of Fig. 7 concerns mainly the first iterations. It is evident that once one chooses the centrality index from which to start, the trajectories to the limit point are different: the trajectories highlight the form that Icentr gives to the set of vectors with norm 1 (the slower the convergence, the softer the form). Because the slowest trajectory changes according to the edge weights, their importance becomes evident. E.g., in Fig. 7, Eigenvector centrality is the slowest in the DEW case.

When we adopt the descriptive statistics point of view, Fig. 8 shows that the mean value and the standard deviation behave opposite each other and that the number of iterations to get the mean value and the standard deviation of the Perron-Frobenius eigenvector is

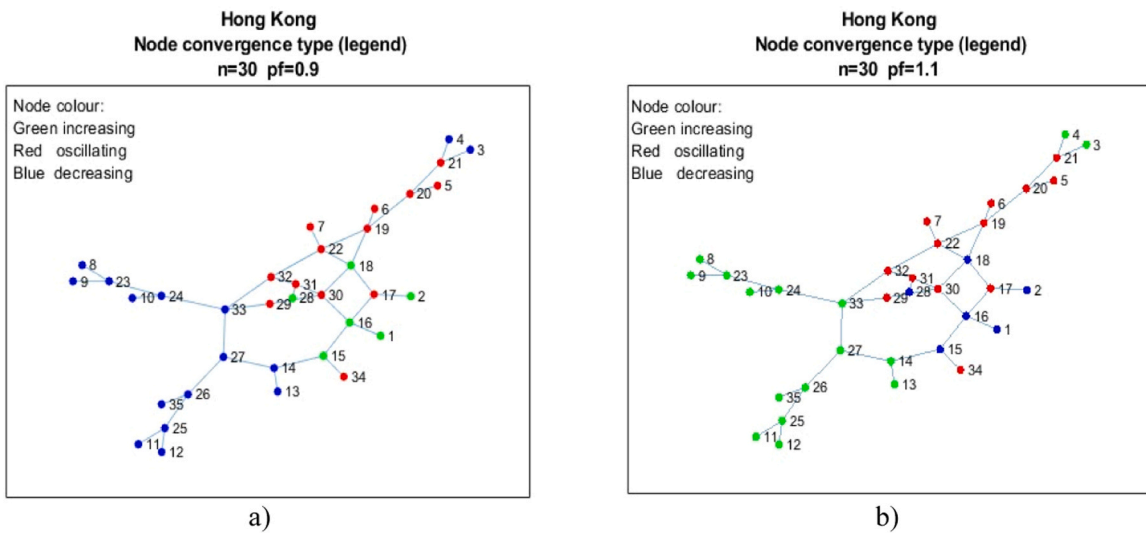


Fig. 10. Results on the convergence type of nodes when starting from the perturbed normalized Perron-Frobenius eigenvector in Hong Kong metro network. On the left (a), we decrease the value of node 30 by 10%. (pf = 0.9) On the right (b), we increase the value of the same node by 10% (pf = 1.1). It is evident that the convergence type of nodes switches from decreasing to increasing, and conversely, whilst the oscillating nodes are the same in the two cases. We have the same feature even in the case of different percentages for pf. For Hong Kong metro network, from 2 to 5 iterations are needed to recover the normalized Perron-Frobenius eigenvector after the perturbation.

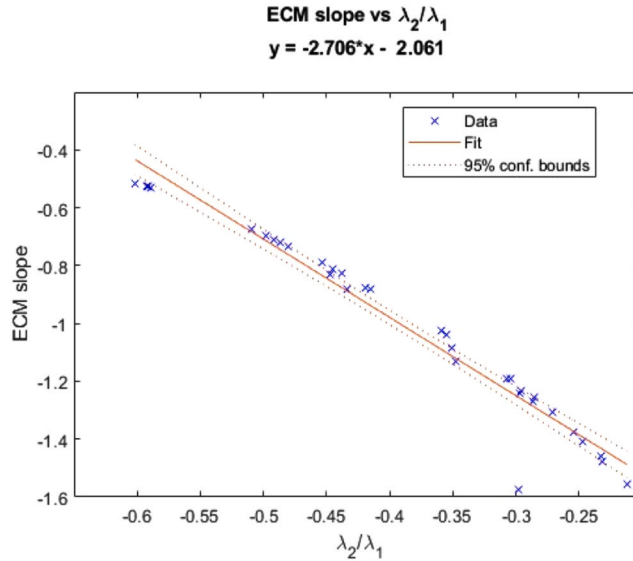


Fig. 11. Plot of the ratio of the two greatest eigenvalues and the average slope of the log of the norm of the difference between the Icentr iterates and the Perron-Frobenius eigenvector, its points are linearly aligned with a very good approximation. This strongly confirms that the rate of convergence of the Icentr iterates to the Perron-Frobenius eigenvector is well described by the ratio between the two largest eigenvalues.

related to the number of iterations so that the logarithm of the norm of the difference becomes linear. Now, we show that this is a general feature. We set $E(Y_t)$, $\sigma(Y_t)$, $E(v)$ and $\sigma(v)$ the mean value and the standard deviation of the Icentr iterates and of the Perron-Frobenius positive eigenvector, respectively. If $Y_t(i)$ is the value of Y_t at the node i , it holds

$$\sigma^2(Y_t) = \frac{\sum_{i=1}^N (Y_t(i) - E(Y_t))^2}{N} = \frac{1}{N} \left(\|Y_t\|^2 - 2NE(Y_t)^2 + NE(Y_t)^2 \right) = \frac{1}{N} - E(Y_t)^2. \tag{17}$$

Eq. (17) explains why the mean value and standard deviation behave oppositely. Furthermore, we get that the mean value and the standard deviation of each iterate are upper bounded by.

Finally, we provide a bound on the average value $E(Y_t)$ in terms of $E(v)$ and $\|Y_t - v\|$. Indeed, for each node i , we have

$$|Y_t(i) - v(i)| \leq \|Y_t - v\|. \tag{18}$$

Eq. (18) can be rewritten as

$$v(i) - \|Y_t - v\| \leq Y_t(i) \leq v(i) + \|Y_t - v\| \tag{19}$$

By taking the average value, we get

$$E(v) - \|Y_t - v\| \leq E(Y_t) \leq E(v) + \|Y_t - v\|. \tag{20}$$

For t large enough, we have that $E(Y_t) \in [E(v) - c_1 e^{-m_1 t}, E(v) + c_1 e^{-m_1 t}]$. Because the exponential approaches zero extremely quickly, the difference between the means of the Icentr iterate and of the Perron-Frobenius eigenvector is quite negligible after a few iterates. Also for the average, it is interesting to look at the first iterations: it is evident that for some choices of the starting point, the average of the Icentr iterates is smaller than the one of the Perron-Frobenius eigenvector, and larger for others. However, the second iterate seems to be crucial, because the inequality that it verifies is the same verified by all the next ones, as witnessed by Fig. 8 for the Hong Kong network.

As last remark, if we consider the norm of the difference between two consecutive Icentr iterates, we get results that look like the ones we have just described, and so we do not repeat the analysis for ICM method.

Finally, we consider all networks in the dataset, with the aim of finding an index able to compare the dynamical properties of each network. From Tables 2 and 3, it emerges that no centrality index from which we start the Icentr computation has properties that are worse or better than the others, and the statistical properties do not help as well. On the other hand, we have that the convergence of Icentr iterates to the Perron-Frobenius positive normalized eigenvector is exponential. From Fig. 7, the convergence rate seems to be independent of the centrality index from which one starts, at least in the case of Hong Kong network. This is the case for all networks. However, mainly because of numerical approximations, the slope is not constant. To reduce the impact of such fluctuations, we compute the average slope. Moreover, from a theoretical point of view, the convergence rate should be related to the ratio between the modulus of the second largest eigenvalue and the Perron-Frobenius eigenvalue of the matrix M constructed in Theorem 1. So, we have computed the average of the slope of $\log\|Y_t - v\|$ and compared with the eigenvalue ratio. It is worth noting that the second largest eigenvalue is real and negative for every considered network.

From a computational standpoint, calculating the average slope necessitates the computation of numerous I_{centr} iterates, because the first ones cannot be used (see Fig. 7 and the related comments in Section 4.2), and the useful ones must be averaged. On the contrary, the matrix M must be computed before the computation of I_{centr} iterates, and so its eigenvalues are known. Moreover, they do not depend on the centrality index chosen to start the computation. For those reasons, we propose the ratio between the two largest eigenvalues of M as an index able to describe the dynamical properties of networks: the closer to 0 the absolute value of the eigenvalue ratio, the faster the convergence of the I_{centr} iterates to the positive normalized Perron-Frobenius eigenvector. In Fig. 12, we plot the eigenvalue ratios against the number of nodes of the network in the UEW case. For the two other edge weights, we get similar figures. We report in Appendix 3 the eigenvalue ratios for all networks in the dataset, for the three edge weights. The networks change their dynamical properties when we change the edge weight, and this highlights their importance, once again. Moreover, if we rank the networks according to the eigenvalue ratio, we find that Buenos Aires, in the UEW case and Montreal in the DEW and SEW cases have the best dynamical performance, whereas Seoul in the UEW and DEW cases, and Osaka in the SEW case have the worst dynamical performance.

6. Conclusions

In this paper we have addressed the evaluation of networks from a dynamical perspective without changing the network topology, focusing on underground transportation networks to fill a gap in the current research. The approach we propose can be applied to other types of networks as well. The main tool is the centrality index I_{centr} , which was introduced in Mussone, Viseh, and Notari [1]. This index accepts both node weights and edge weights and becomes a dynamical system when we use as node weights the normalized outcome of the index itself, called I_{centr} iterates. As preliminary step, we have computed the matrix M that is equivalent to the I_{centr} computation, and we have proved that it has a positive (real) eigenvalue that is larger than the modulus of all other eigenvalues and called it the Perron-Frobenius eigenvalue. The Perron-Frobenius eigenvector is the only eigenvector with modulus one and positive entries of M . Moreover, we have evaluated the computational complexity of I_{centr} and described an algorithm to efficiently compute it. We have proved that the I_{centr} iterates converge to the Perron-Frobenius eigenvector. The dynamics of a network can be inspected at two levels, namely at node and at network level. Furthermore, we have compared the dynamical properties of different networks.

At node level, we have found that the space of the normalized vector with positive entries from which one starts the computation of I_{centr} iterates is divided in two regions, one containing the Eigenvector centrality, the other containing the Betweenness, Closeness, Degree, and Uniform node weights. The border between the two regions is identified by nodes whose values oscillate at each I_{centr} iterate.

At the network level, we have discovered that after a few iterates, the convergence to the Perron-Frobenius eigenvector is exponential in the number of iterations. Furthermore, the standard deviation and expected value of I_{centr} iterates are strongly related each other, so knowing one is comparable to knowing both.

Finally, we have proved that the rate of convergence of I_{centr} iterates to the Perron-Frobenius eigenvector can be very well described by the ratio between the modulus of the second largest eigenvalue and the Perron-Frobenius eigenvalue of M . The comparison between the dynamical properties of two networks can be done by inspecting the associated ratios: the closer to zero the ratio, the faster the convergence of I_{centr} iterates to the Perron-Frobenius eigenvector.

We have applied the described methodology to graphs representing underground networks of 34 cities around the world. We

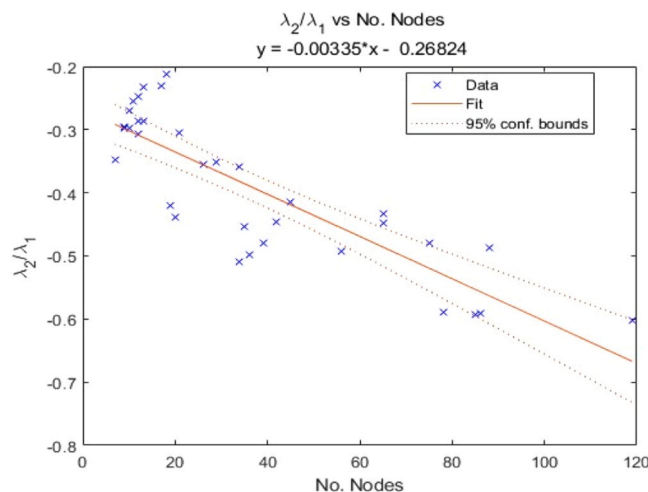


Fig. 12. For the Uniform Edge Weight, the ratio between the two largest eigenvalues of the matrix M is slightly influenced by the number of nodes in the network. Indeed, the slope of the regression line is of the order 3×10^{-3} . Because the points are widely distributed around the regression line, the eigenvalue ratio can identify the dynamical properties of the networks: the closer the absolute value of the ratio to 0, the faster the convergence to the limit point.

computed all needed data and included them into the [Appendices](#) of the present paper, for completeness.

The methodology we have described can be used also to assess the dynamical performance of a network at different phases of development and with edge weights that depend on time, such as the number of passengers at different hours of a day or the number of trains circulating on the edges.

CRedit authorship contribution statement

notari roberto: Writing – original draft, Visualization, Validation, Supervision, Software, Methodology, Investigation, Formal analysis, Data curation, Conceptualization. **Tarek Mudawar:** Writing – original draft, Visualization, Investigation, Data curation. **mussone lorenzo:** Writing – original draft, Visualization, Validation, Supervision, Software, Methodology, Investigation, Formal analysis, Data curation, Conceptualization.

Declaration of Competing Interest

The authors declare that they have no known conflict of interest or personal relationships in any material discussed in this article.

Appendix A. An algorithm for computing I_{centr} and its computational complexity

In this appendix, we provide an algorithm to compute I_{centr} , given the graph and the weights of nodes and edges, from which we evaluate the computational complexity of I_{centr} .

Function I_{centr}

Input:

- graph $G = (V, E)$.
- nw = node weights.
- ew = edge weights.

Output: I_{centr} vector.

```

For  $v \in V$  do
  Nodelevel( $v$ ) = 0
  Nodewithlevel = { $v$ }
  Nodewithoutlevel =  $V \setminus \{v\}$ 
  Edgelist =  $E$ 
  Level=1
  Denomfirst=1
  Denomsecond=2
   $I_{centr}(v)=0$ 
  While Nodewithoutlevel  $\neq \emptyset$  do
    For  $w \in$  Nodewithlevel such that Nodelevel( $w$ ) = Level-1 do
      For  $z \in V$  such that  $\{w, z\} \in$  Edgelist do
        Case Nodelevel( $z$ ) = Level - 1:
           $I_{centr}(v) = I_{centr}(v) + (nw(w) + nw(z)) * ew(w, z) / Denomsecond$ 
        Case Nodelevel( $z$ ) = Level
           $I_{centr}(v) = I_{centr}(v) + nw(z) * ew(w, z) / Denomfirst$ 
        Case  $z \in$  Nodewithoutlevel
          Nodewithlevel = Nodewithlevel  $\cup \{z\}$ 
          Nodewithoutlevel = Nodewithoutlevel  $\setminus \{z\}$ 
          Nodelevel( $z$ ) = Level
           $I_{centr}(v) = I_{centr}(v) + nw(z) * ew(w, z) / Denomfirst$ 
        Endcase
        Edgelist = Edgelist  $\setminus \{\{w, z\}\}$ 
      Endfor
    Endfor
    Level = Level + 1
    Denomfirst = 2 * Denomfirst
    Denomsecond = 2 * Denomsecond
  Endwhile
  For  $\{w, z\} \in$  Edgelist do
     $I_{centr}(v) = I_{centr}(v) + (nw(w) + nw(z)) * ew(w, z) / Denomsecond$ 
  Endfor
Endfor
Return  $I_{centr}$ 
End function

```

It is worth noting that the levels of nodes can be determined also by calculating the distance from the starting node in the topological adjacency matrix. However, this approach does not allow us to understand the complexity of the algorithm.

The correctness of the procedure stems from the following remarks. In the **while do** cycle, we assign a level to each node different

from v and, at the same time, we update $I_{centr}(v)$, according to the following criterium.

If all nodes with level $h - 1$ have been considered, and a node, say w , has level h and is linked to another node z , then only one of the following possibilities occurs: (a) $level(z) = level(w)$, and so we can calculate the contribution of the edge $\{w, z\}$; (b) $level(z) = level(w) + 1$, and again we can calculate the contribution of $\{w, z\}$; (c) z has not jet a level, and so we assign the level $h + 1$ to z and we can calculate the contribution of $\{w, z\}$. Once every node has a level, the only edges that have not been considered yet, link nodes with the largest level, and so we can calculate the contribution of these last edges. The procedure can easily be adapted to compute the matrix \mathbf{M} of the dynamical system.

The computational complexity of the procedure is $O(N^2)$, where N is the number of nodes if the graph is planar, which is common for transportation networks. Indeed, for computing the contribution of each edge, we use two multiplications. Moreover, the procedure updates the two possible denominators as many times as the number of levels, and so it performs two times the number of levels multiplications, too. In the case the graph is a chain, that is the worst case, there are $N - 1$ levels, and so the procedure executes about $2N + 2|E|$ products, at most (E is the number of edges). Since for planar graphs, the number of edges is at most $3N - 6$, we get that the complexity of the computation of the I_{centr} value at a node is $8N - 12$. As the procedure repeats the computation for each node, the complexity of the procedure is quadratic in the number of nodes.

Appendix B. Number of iterations for the networks in the dataset

In this appendix, we report the number of iterations for the networks in the dataset, for the two methods (ECM and ICM), the three edge weights (UEW, DEW, SEW) and the five centrality indices from which we start I_{centr} computation (Betweenness, Closeness, Degree, Eigenvector, Uniform).

Table B1

Number of iterations to satisfy the condition $\log\|Y_t - \bar{v}\| < 10^{-5}$ where Y_t is the normalized t -th I_{centr} iterate and \bar{v} is the Perron-Frobenius eigenvector with norm 1 (ECM method), for centrality index as starting point, and edge weight.

Underground Networks	Betweenness			Closeness			Degree			Eigenvector			Uniform		
	UEW	DEW	SEW	UEW	DEW	SEW	UEW	DEW	SEW	UEW	DEW	SEW	UEW	DEW	SEW
Athens	8	31	14	6	29	12	7	27	13	7	24	13	7	25	12
Barcelona	13	30	15	12	30	15	13	24	15	13	33	20	13	28	17
Beijing	18	77	25	17	68	24	17	89	28	18	105	35	17	79	26
Berlin	14	17	16	12	17	16	11	15	14	14	18	17	11	17	16
Boston	8	43	28	8	45	28	8	49	21	9	62	28	9	46	27
Brussels	9	11	11	7	10	10	7	10	10	8	9	10	7	9	10
Bucharest	8	11	10	7	9	8	8	10	9	7	10	9	8	9	8
Buenos Aires	7	13	9	6	12	9	6	11	8	6	14	11	6	12	9
Cairo	7	23	15	6	21	13	7	18	13	6	17	12	6	19	12
Chicago	10	17	14	9	15	14	10	14	14	9	18	17	10	14	12
Delhi	12	13	13	11	13	14	11	10	14	9	15	17	12	13	13
Hong Kong	13	30	13	12	27	14	12	25	14	13	31	17	13	27	10
Lisbon	7	12	9	5	12	9	7	12	9	6	11	9	6	11	9
London	13	31	14	13	32	18	12	32	16	13	40	21	13	31	17
Lyon	9	15	11	5	13	9	8	14	11	8	13	10	7	13	10
Madrid	14	66	28	13	70	23	12	63	29	14	66	36	12	68	27
Marseilles	11	16	13	8	13	11	10	14	12	9	13	11	9	13	11
Mexico City	10	19	13	11	17	13	11	15	13	13	21	17	12	16	13
Milan	8	17	11	7	17	11	7	15	11	8	19	13	7	17	10
Montreal	8	10	10	5	8	8	8	9	10	7	9	9	7	9	9
Moscow	11	21	19	11	21	19	10	18	15	12	22	22	11	21	18
New York	19	29	26	18	29	26	17	27	25	19	29	28	18	29	26
Osaka	15	34	35	14	37	14	13	33	35	15	34	42	14	36	33
Paris	18	37	23	17	36	23	16	33	22	17	47	30	17	34	23
Prague	8	15	13	4	13	11	7	13	11	7	11	10	7	13	11
Rome	9	23	17	7	20	15	8	20	16	8	18	15	7	19	15
Saint Petersburg	7	14	10	5	13	9	7	11	9	7	16	11	6	13	9
Seoul	21	293	33	20	286	32	19	252	27	22	291	34	20	284	31
Shanghai	14	22	18	13	22	18	13	20	17	14	24	19	13	21	18
Singapore	9	14	12	7	14	11	7	12	11	8	15	13	8	14	9
Stockholm	12	26	19	12	25	18	11	26	18	13	34	22	12	25	19
Tokyo	12	20	13	9	20	14	8	18	13	10	22	17	9	20	13
Toronto	9	23	17	7	19	14	8	20	15	7	25	18	7	17	13
Washington	10	28	12	9	28	12	8	25	11	9	30	13	9	26	12

Table B2

Number of iterations to satisfy the condition $\log\|Y_{t+1} - Y_t\| < 10^{-5}$ where Y_t is the normalized t-th Icentr iterate (ICM method), for centrality index as starting point, and edge weight.

Underground Networks	Betweenness			Closeness			Degree			Eigenvector			Uniform		
	UEW	DEW	SEW	UEW	DEW	SEW	UEW	DEW	SEW	UEW	DEW	SEW	UEW	DEW	SEW
Athens	9	34	16	7	31	14	8	29	15	8	26	14	8	27	14
Barcelona	13	28	15	12	27	15	13	22	15	13	31	20	13	25	16
Beijing	17	59	23	16	49	22	16	70	25	17	87	33	17	60	24
Berlin	14	17	16	12	17	16	11	15	14	14	18	17	11	17	16
Boston	9	35	26	9	37	26	9	41	19	10	54	26	9	38	25
Brussels	10	13	13	8	11	11	9	11	12	9	11	11	8	11	11
Bucharest	9	12	11	8	10	9	9	11	10	8	11	10	8	10	9
Buenos Aires	8	14	11	7	13	9	7	12	10	7	14	12	7	13	10
Cairo	8	25	17	7	23	15	8	20	14	7	19	14	7	20	14
Chicago	11	19	14	10	16	14	10	15	14	10	18	17	10	16	12
Delhi	13	13	13	12	13	14	12	10	14	9	15	17	12	13	13
Hong Kong	13	27	13	13	24	14	12	22	14	14	28	17	13	24	10
Lisbon	9	14	10	6	13	11	8	13	11	7	12	10	7	12	10
London	14	27	14	13	29	17	12	28	16	13	37	20	13	28	17
Lyon	10	17	13	7	14	11	9	15	12	9	14	11	9	14	11
Madrid	14	56	25	13	59	21	12	53	27	14	56	33	12	57	25
Marseilles	12	17	15	9	15	12	11	16	13	10	15	13	10	14	12
Mexico City	10	18	13	12	17	13	11	14	13	13	21	17	12	16	13
Milan	8	17	11	7	17	12	8	16	11	8	18	14	8	16	10
Montreal	10	11	11	6	9	9	9	11	11	9	10	10	8	10	10
Moscow	11	20	18	11	20	18	11	18	14	12	21	21	11	20	17
New York	19	27	25	18	27	24	16	25	23	19	27	26	17	27	24
Osaka	15	31	31	14	34	14	13	30	31	15	31	39	14	33	29
Paris	17	32	21	16	31	21	15	28	21	16	42	28	16	30	21
Prague	9	17	14	5	14	12	8	14	13	8	13	12	8	14	12
Rome	10	25	19	8	22	17	9	22	18	9	20	16	8	21	16
Saint Petersburg	8	15	11	6	14	10	8	12	10	8	16	11	7	13	10
Seoul	20	209	30	19	201	29	18	167	24	21	206	31	19	200	28
Shanghai	15	21	18	13	21	18	13	19	17	14	23	19	13	21	18
Singapore	10	14	12	8	15	11	8	12	11	9	15	14	8	14	9
Stockholm	12	24	18	12	23	17	12	24	17	13	31	21	12	23	18
Tokyo	12	19	13	9	20	14	9	17	13	10	21	17	10	19	13
Toronto	10	22	17	8	20	14	9	20	15	9	24	18	8	18	14
Washington	11	26	12	10	26	12	9	24	12	10	28	13	10	24	12

Appendix C. Ratios between the two largest eigenvalues for the networks in the dataset

Here, we report the ratios between the modulus of the second largest eigenvalue and the Perron-Frobenius eigenvalue for all networks in the dataset, and the three edge weights, so to easily compare the dynamical properties of the networks.

Table C1

Ratio of the two greatest eigenvalues of matrix M for the three cases of edge weights for all the networks in the dataset.

Underground Networks	λ_2/λ_1		
	UEW	DEW	SEW
Athens	-0,28697	-0,69662	-0,45527
Barcelona	-0,49813	-0,70577	-0,56682
Beijing	-0,58945	-0,89218	-0,69786
Berlin	-0,51000	-0,53425	-0,52307
Boston	-0,35119	-0,82522	-0,66566
Brussels	-0,29617	-0,38428	-0,39849
Bucharest	-0,28587	-0,38551	-0,33808
Buenos Aires	-0,21211	-0,44632	-0,37254
Cairo	-0,24675	-0,61598	-0,47547
Chicago	-0,41962	-0,53655	-0,51158
Delhi	-0,41493	-0,45328	-0,50577
Hong Kong	-0,45329	-0,71262	-0,50412
Lisbon	-0,23232	-0,42841	-0,34882
London	-0,47997	-0,73056	-0,5808
Lyon	-0,27052	-0,46478	-0,37432

(continued on next page)

Table C1 (continued)

Underground Networks	λ_2/λ_1		
	UEW	DEW	SEW
Madrid	-0,4921	-0,84665	-0,70413
Marseilles	-0,34725	-0,47546	-0,41488
Mexico City	-0,44522	-0,57626	-0,50404
Milan	-0,30427	-0,53381	-0,43012
Montreal	-0,25398	-0,32250	-0,33242
Moscow	-0,43368	-0,59124	-0,58106
New York	-0,59235	-0,68739	-0,66178
Osaka	-0,48026	-0,72418	-0,75032
Paris	-0,59124	-0,77454	-0,66867
Prague	-0,29754	-0,44853	-0,39818
Rome	-0,29712	-0,6081	-0,52057
Saint Petersburg	-0,23155	-0,49314	-0,41197
Seoul	-0,60171	-0,96245	-0,71183
Shanghai	-0,48682	-0,61303	-0,55055
Singapore	-0,35869	-0,46718	-0,41821
Stockholm	-0,43792	-0,7032	-0,61159
Tokyo	-0,44728	-0,59488	-0,4991
Toronto	-0,30701	-0,62671	-0,52495
Washington	-0,35456	-0,68044	-0,42015

Data availability

Data will be made available on request.

References

- [1] L. Mussone, H. Viseh, R. Notari, Novel centrality measures and applications to underground networks, *Phys. A: Stat. Mech. Appl.* 589 (2022) 126595, <https://doi.org/10.1016/j.physa.2021.126595>.
- [2] S. Derrible, C. Kennedy, The complexity and robustness of metro networks, *Physica A* 389 (2010) 3678–3691, <https://doi.org/10.1016/j.physa.2010.04.008>.
- [3] D. King, A. Aboudina, A. Shalaby, Evaluating transit network resilience through graph theory and demand-elastic measures: case study of the Toronto transit system, *J. Transp. Saf. Secur.* 12 (7) (2019) 924–944, <https://doi.org/10.1080/19439962.2018.1556229>.
- [4] Y. Yang, Y. Liu, M. Zhou, F. Li, C. Sun, Robustness assessment of urban rail transit based on complex network theory: a case study of the Beijing Subway, *Saf. Sci.* 79 (2015) 149–162, <https://doi.org/10.1016/j.ssci.2015.06.006>.
- [5] O. Cats, G.J. Koppenol, M. Warnier, Robustness assessment of link capacity reduction for complex networks: application for Public Transport Systems, *Reliab. Eng. Syst. Saf.* 167 (2017) 544–553, <https://doi.org/10.1016/j.res.2017.07.009>.
- [6] D. Zhang, F. Du, H. Huang, F. Zhang, B. Ayyub, M. Beer, Resiliency assessment of urban rail transit networks: Shanghai metro as an example, *Saf. Sci.* 106 (2018) 230–243, <https://doi.org/10.1016/j.ssci.2018.03.023>.
- [7] L. Sun, Y. Huang, Y. Chen, L. Yao, Vulnerability assessment of urban rail transit based on multistatic weighted method in Beijing, China, *Transp. Res. Part A: Policy Pract.* 108 (2018) 12–24, <https://doi.org/10.1016/j.tra.2017.12.008>.
- [8] E. Estrada, The communicability distance in graphs, *Linear Algebra Appl.* 436 (11) (2012) 4317–4328, <https://doi.org/10.1016/j.laa.2012.01.017>.
- [9] L. Cavallaro, P. De Meo, G. Fiumara, A. Liotta, On the sensitivity of centrality measures, *PLoS One* 19 (5) (2024) 1–25, <https://doi.org/10.1371/journal.pone.0299255>.
- [10] C. Ducruet, L. Beauguitte, Spatial science and network science: review and outcomes of a complex relationship, *Netw. Spat. Econ.* 14 (2014) 297–316, <https://doi.org/10.1007/s11067-013-9222-6>.
- [11] Y. Meng, Q. Qi, J. Liu, W. Zhou, Dynamic evolution analysis of complex topology and node importance in Shenzhen metro network from 2004 to 2021, *Sustainability* 14 (12) (2022) 7234, <https://doi.org/10.3390/su14127234>.
- [12] L. Zhang, J. Lu, B. Fu, S. Li, Dynamics analysis for the hour-scale based time-varying characteristic of topology complexity in a weighted urban rail transit network, *Phys. A: Stat. Mech. Appl.* 628 (2019) 121280, <https://doi.org/10.1016/j.physa.2019.121280>.
- [13] B. Leng, X. Zhao, Z. Xiong, Evaluating the evolution of subway networks: evidence from Beijing Subway Network, *Europhys. Lett.* 105 (5) (2014) 58004, <https://doi.org/10.1209/0295-5075/105/58004>.
- [14] A. Zahoor, I.A. Gillani, Ju Bashir, A review of temporal networks: operations and applications, *Rev. Socionetw. Strat.* 19 (2025) 183–236, <https://doi.org/10.1007/s12626-025-00187-5>.
- [15] Yunlong Peng, Han Li, Xu Han, Time series forecasting based on temporal networks evolution and dynamic constraints, *IEEE Access* 13 (2025) 99160–99169, <https://doi.org/10.1109/ACCESS.2025.3577499>.
- [16] A. Ali, I. Ullah, Zongze Wu, Jiangqiang Li, Xiaoshan Bai, An attention-driven spatio-temporal deep hybrid neural networks for traffic flow prediction in transportation systems, *IEEE Trans. Intell. Transp. Syst.* 26 (9) (2025) 14154–14168, <https://doi.org/10.1109/TITS.2025.3540852>.
- [17] W.E. Arnoldi, The principle of minimized iterations in the solution of the matrix eigenvalue problem, *Q. Appl. Math.* 9 (1951) 17–29, <https://api.semanticscholar.org/CorpusID:115852469>.
- [18] C. Lanczos, An iteration method for the solution of the eigenvalue problem of linear differential and integral operators, *J. Res. Natl. Bur. Stand.* 45 (1950) 255–282, <https://doi.org/10.6028/jres.045.026>.
- [19] A.S. Householder, The theory of matrices in numerical analysis, *Am. Math. Mon.* 73 (10) (1966) 1142, <https://doi.org/10.2307/2314680>.
- [20] N. Meghanathan, Using spectral radius ratio for node degree to analyze the evolution of scale free networks and small world networks, *Comput. Sci.: Soc. Inf. Netw.* (2015), <https://doi.org/10.48550/arXiv.1504.02504>.
- [21] C. Chen, H. Tong, On the eigen-functions of dynamic graphs: fast tracking and attribution algorithms: eigen-functions of dynamic graphs, *Stat. Anal. Data Min.: ASA Data Sci. J.* 10 (2016) 121–135, <https://doi.org/10.1002/sam.11310>.
- [22] L.C. Freeman, A set of measures of centrality based on betweenness, *Sociometry* 40 (1) (1977) 35–41, <https://doi.org/10.2307/3033543>.
- [23] M. Barthélemy, Betweenness centrality in large complex networks, *Eur. Phys. J. B* 38 (2004) 163–168, <https://doi.org/10.1140/epjb/e2004-00111-4>.

- [24] U. Brandes, A faster algorithm for betweenness centrality, *J. Math. Sociol.* 25 (2) (2001) 163–177, <https://doi.org/10.1080/0022250X.2001.9990249>.
- [25] A. Bavelas, Communication patterns in task- oriented groups, *J. Acoust. Soc. Am.* 22 (1950) 725–730, <https://doi.org/10.1121/1.1906679>.
- [26] M. Piraveenan, N.B. Saripada, Transportation centrality: quantifying the relative importance of nodes in transportation networks based on traffic modeling, *IEEE Access* 11 (2023) 14–34, <https://doi.org/10.1109/ACCESS.2023.3339121>.
- [27] P. Bonacich, Factoring and weighting approaches to status scores and clique identification, *J. Math. Sociol.* 2 (1) (1972) 113–120, <https://doi.org/10.1080/0022250X.1972.9989806>.
- [28] R. Von Mises, H. Pollaczek-Geiringer, Praktische verfahren der gleichungsauflosung, *Z. Angew. Math. Mech.* 9 (1929) 58–77, <https://doi.org/10.1002/zamm.19290090105>.
- [29] A.S. Householder, *The Theory of Matrices in Numerical Analysis*, Blaisdell Publishing Company, 1964.
- [30] J. Von Neumann, *Functional Operators, Volume 1: Measures and Integrals*, Princeton University Press, 1950.